NASA Technical Memorandum 103854

IN-47
48765
P.15

Aerodynamic Design of Gas and Aerosol Samplers for Aircraft

Paul T. Soderman, Nathan L. Hazen,
and William H. Brune

(NASA-TM-103854) AERODYNAMIC DESIGN OF GAS AND AEROSOL SAMPLERS FOR AIRCRAFT (NASA) 15 p CSCL 04B

N92-13522

Unclas
G3/47 0049765

September 1991

National Aeronautics and
Space Administration

NASA Technical Memorandum 103854

Aerodynamic Design of Gas and Aerosol Samplers for Aircraft

Paul T. Soderman, Ames Research Center, Moffett Field, California
Nathan L. Hazen, Harvard University, Cambridge, Massachusetts
William H. Brune, Pennsylvania State University, University Park, Pennsylvania

September 1991

National Aeronautics and
Space Administration

Ames Research Center
Moffett Field, California 94035-1000

Summary

The aerodynamic design of airborne probes for the capture of air and aerosols is discussed. Emphasis is placed on the key parameters that affect proper sampling, such as inlet-lip design, internal duct components for low pressure drop, and exhaust geometry. Inlet designs that avoid sonic flow conditions on the lip and flow separation in the duct are shown. Cross-stream velocities of aerosols are expressed in terms of droplet density and diameter. Flow curvature, which can cause aerosols to cross streamlines and impact on probe walls, can be minimized by means of a proper inlet shape and proper probe orientation, and by avoiding bends upstream of the test section. A NASA panel code called PMARC has been used successfully to compute streamlines around aircraft and probes, as well as to compute the local velocity and pressure distributions in inlets. An NACA 1–series inlet with modified lip radius has been used for the airborne capture of stratospheric chlorine monoxide at high altitude and high flight speed. The device has a two-stage inlet that decelerates the inflow with little disturbance to the flow through the test section. Diffuser design, exhaust hood design, valve loss, and corner vane geometry are discussed.

Nomenclature

A_i	diffuser inlet flow area, m^2
A_o	diffuser outlet flow area, m^2
b	wing span, m
c	wing chord, m
$\bar{c}$	wing aerodynamic chord = $\frac{1}{S}\int_{-b/2}^{b/2} c^2\,(y)\,dy$, m
C_L	wing lift coefficient
d	duct diameter, m
d_p	diameter of aerosol droplet or particle, m
K_v	total pressure loss coefficient, $\Delta p/q$
l_{dif}	streamwise length of diffuser, m
L	wing lift, N
M	Mach number
M_d	average Mach number of airflow in duct
M_o	aircraft Mach number
p	local static pressure, N/m^2
p_o	free-stream static pressure, N/m^2
P	static-pressure coefficient, $\frac{p-p_o}{q}$
q	free-stream dynamic pressure, N/m^2
r	distance from vortex core to induced streamline, or distance from wing quarter chord to upwash location (fig. 1), m
Re	Reynolds number based on duct diameter, $\rho V_d\, d/\mu$
S	wing area, m^2
V_d	average velocity in a duct, m/sec
V_{max}	maximum velocity in a duct, m/sec
V_o	velocity of aircraft, m/sec
V_r	particle velocity perpendicular to fluid streamline, m/sec
V_t	particle velocity tangent to fluid streamline, m/sec
V_1	velocity in sampler primary inlet, m/sec
V_2	velocity in sampler secondary inlet, m/sec
V_3	velocity in sampler test section, m/sec
w	wing upwash or downwash velocity, m/sec
W	aircraft weight, N
x	distance in boundary layer parallel to duct, m
α_i	angle of attack induced by wing upwash, rad
α_w	angle of one diffuser wall relative to duct centerline, deg
Γ	vortex strength, m^2/sec
Δp	total pressure loss at duct component, N/m^2
Θ	upwash angle (fig. 1), deg
μ	viscosity of air, kg/m sec
ν	kinematic viscosity of air, m^2/sec
ρ	air density, kg/m^3
ρ_p	aerosol droplet or particle density, kg/m^3
ω	vortex rotation rate, rad/sec

Introduction

High-altitude sampling of atmospheric chemistry has been accomplished for many years by using rocket-launched parachute drops and balloon drops (Anderson, 1975). More recently, the authors have been involved in airborne sampling using the NASA ER-2 aircraft, primarily to investigate the role of free radical chlorine monoxide (ClO) in ozone depletion in the stratosphere (Brune et al.,

1988). Requirements for smooth, regulated airflow to the chemistry analysis section of the experiments have led to work in inlet- and internal-duct aerodynamic design. For example, it is often necessary in airborne experiments to decelerate the airflow smoothly so as to minimize turbulence in the sampled airstream. In an air sampler, turbulence could allow wall interactions that would alter the abundance of the gas being investigated. Similar flow constraints are required for aerosol sampling (Huebert et al., 1990).

Fortunately, there is a large body of literature on inlet- and internal-duct design. Aerodynamicists have been concerned for many years about aircraft fluid mechanics related to smooth inflow to engines, flow separation, shock formation, boundary-layer control, fuselage streamlines, wing upwash, internal duct losses, corner vane design, pressure probe design, and so on. All of these subjects are important to the design of airborne sampling systems for gas and aerosols and will be discussed.

With respect to aerosol sampling, the two most important aerodynamic constraints are (1) minimization of the inflow streamline curvature, since aerosols tend to cross curved streamlines because of inertia (an action that leads to inaccurate estimates of aerosol concentration); and (2) elimination of turbulence, because turbulence leads to wall collisions and removal of aerosols from the airstream (Huebert et al., 1990). It is also assumed that it is often necessary to decelerate the flow for the gas-analysis system. This paper will focus on design ideas that affect those aerodynamic goals.

Aerosol Motion

Aerosols or particles following a curved streamline experience a centrifugal force that tends to drive the particles across fluid streamlines. This is a common problem in laser velocimetry, where flow velocities, which are deduced from particle motion, can be in error if the particles do not faithfully follow fluid streamlines. Likewise, curved streamlines can cause deposition of aerosols on probe walls and thereby lead to erroneous concentration measurements.

A curved streamline can be thought of as a rotational field like that induced by a vortex where all streamlines are circumferential. The tangential velocity is

$$V_t = r\omega \tag{1}$$

where ω is the vortex rotation rate necessary to produce V_t, and r is the distance from the vortex center to the streamline. Thus, r is the radius of a circle tangent to the curved streamline at the region of interest. The centrifugal force creates a radial velocity experienced by a particle (Durst et al., 1976):

$$V_r = \frac{r\omega^2 d_p^2 \rho_p}{18\mu} \tag{2}$$

Thus, the radial velocity depends on the particle density and on the diameter squared. The radial displacement can then be computed for a given flow curvature. For high streamline curvature, particles must be very small in order to have a small radial velocity and displacement.

Inlet Design

Probes for airborne aerosol samplers must capture the airflow smoothly over a small but significant range of inflow angles. Inflow angles change during flight because of changes in aircraft airspeed and in angle of attack as fuel is burned or as altitude is varied.

Probe orientation can be optimized to coincide with local streamlines. Estimates can be made of streamline direction anywhere near the aircraft if the aircraft geometry, airspeed, and wing lift are known. Approximate estimates of wing upwash velocity w and induced angle of attack α_i can be made using a simple vortex-line modeling of the wing, as illustrated in figure 1. The vortex strength is

$$\Gamma = \frac{L}{\rho b V_o} \tag{3}$$

and the upwash velocity ahead of the wing is

$$w = \frac{\Gamma}{2\pi r} \tag{4}$$

In level flight, aircraft lift equals weight, so the lift coefficient is given by

$$C_L = \frac{L}{qS} = \frac{W}{qS} \tag{5}$$

and the induced angle of attack is

$$\alpha_i = \frac{w}{V_o}\cos\theta = \frac{C_L \bar{c}\cos\theta}{4\pi r} \tag{6}$$

for small values of w.

The above equations gave a value of 3.9° for the ER-2 aircraft wing pod station 3 m ahead of the wing quarter chord. Thus, a probe at that location would be oriented 3.9° downward for alignment with the local flow.

Detailed flow-field streamlines are better computed using computer panel methods. We have used the NASA Ames PMARC code, which is a low-order, potential-flow panel code (Ashby et al., 1990). Figure 2 shows, for example, streamlines computed near an isolated ER-2 wing pod using PMARC. These streamlines illustrate how far a given probe must project ahead of the pod to capture

airflow upstream of flow curvature. For the probe location noted in figure 2, the inlet was located 46 cm ahead of the wing pod to avoid flow curvature. Similar analyses can be used to estimate streamlines along the aircraft fuselage for various flight conditions.

The requirement that a probe accept airflow over a range of inflow angles leads to the further requirement of inlets with a finite lip thickness. Thin inlet lips function well for axial inflow, but off-axis inflow will separate at the probe leading edge. NACA put considerable work into testing aircraft cowlings during the 1940s, primarily to control velocities at engine inlets so as to avoid shock formations. This is also a problem for the ER-2 and for other aircraft that must fly at high subsonic Mach numbers to attain high altitudes. Local flow accelerations around inlets can cause the flow to go supersonic, even though the aircraft flight speed is subsonic. Shock waves on or near the inlet can adversely influence the flow into the inlet, especially if the shocks oscillate.

The stream tube captured by the probe will be smaller than the duct diameter if the duct velocity is lower than the flight speed, and the stream tube will be larger than the duct diameter if the duct velocity is greater than the flight speed, as illustrated in figure 3. In the first case, the stagnation point will be inside the inlet, and the flow that is not captured will flow out around the lip. As the duct velocity increases, the stagnation point will move forward. Figure 4 shows various stagnation points on an inlet for several values of flight Mach number and for a fixed duct Mach number of 0.85. At low flight Mach number and at high duct speed, the captured flow along the surface must accelerate from the stagnation point high on the nose and flow around the lip and into the duct. This could lead to flow separation. Conversely, a high flight Mach number and low duct Mach number would force the air that is not captured to flow from the stagnation point inside the inlet forward around the lip. Flow separation or sonic flow could result on a sharp or otherwise poorly shaped inlet.

Nichols et al. (1949) and Baals et al. (1948) generated a large data base that shows how NACA 1–series inlet shapes (fig. 5) delay sonic flow and flow separation for a range of flight Mach numbers and for a range of duct-velocity–to–flight-velocity ratios. Re (1975) presented further performance studies of the NACA 1–series inlets. The NACA 1-55-100 inlet shape was chosen for the inlets of the stratospheric sampler used in the ER-2 aircraft over Antarctica (Brune et al., 1989). However, the NACA lip radius was increased to 6.35 mm after discussions with an aircraft manufacturer. (Conversation with Don Nelson of Lockheed Aircraft Co., 1986.) The slightly thicker inlet lip is of a more conservative design than the NACA lip in terms of prevention of flow separation from off-axis flow.

The NACA 1–series geometry is given in figure 6. (The series designation code is explained in the figure.) The NACA 1-55-100 inlet does not induce shock formation or flow separation, even at the ER-2 flight Mach number of 0.7 and at moderate angles of attack of the probe.

More recently, Luidens et al. (1979) have done optimization studies aimed at finding the shortest, thinnest lip that will turn the flow into the inlet at low-speed conditions without flow separation anywhere in the inlet. This results in an elliptical lip. Figure 7 shows the important geometric parameters—fineness ratio and contraction ratio. At duct–to–free-stream-velocity ratios of 1, the flow will stay attached to the lip up to an angle of 28° (Luidens and Abbott, 1976). At lower values of duct–to–free-stream-velocity ratio, the separation angle is much lower (Baals et al.,1948).

In summary, design guides exist for the design of inlet lips and diffusers for low-speed (elliptical lips) and high-speed flight (NACA 1–series). The design should result in thin, but not sharp, lips that can turn off-axis flow into the duct and decelerate the flow by diffusion as it moves downstream, without any flow separation.

Dual Intake

The design of the inlet shape for the ClO sampler flown on the ER-2 was complicated by the requirement that the flow decelerate smoothly from a flight velocity of about 200 m/sec to a test-section velocity of 20 m/sec. That large deceleration is equivalent to a blockage seen by the inflow that causes the air to spill out and around the inlet. Flow acceleration around the inlet outer surface would cause the flow to go sonic and thereby generate shock waves that could oscillate and perturb the flow into the duct. The studies of Nichols et al. (1949) and Baals et al. (1948) indicated that no inlet was found that could handle such a large flow deceleration and spillage without generating external shock waves at the aircraft flight speed of 200 m/sec.

Therefore, a two-stage inlet was devised as shown in figure 8. The idea is that the first (primary) inlet would capture and decelerate a stream tube to 30% of the free-stream velocity or 60 m/sec, and that the second (secondary) inlet would capture the center core of the primary stream tube and decelerate it to 33% of the primary duct velocity, or to a nominal 20 m/sec. The excess flow from the primary duct bypasses the test section and is dumped. Because of the modest decelerations, shock-wave generation would be avoided on both inlets. In addition, the boundary layer in the primary duct would not enter the secondary duct. At the secondary inlet, a new boundary layer would commence but would not have a

chance to grow much in the short distance it traveled to the test section. The primary inlet was designed to accept flow that was off-axis by about 6° or less without flow separation, so turbulence would not enter the center of the duct. (The actual off-axis flow angle that initiates flow separation has not been confirmed.) The secondary inlet would only see on-axis flow.

Analysis of the two inlets in terms of velocity ratios V_d/V_o and critical Mach numbers (Baals et al., 1948) led to the adoption of the NACA 1-55-100 inlet shape with modified lip radius for both the primary and secondary inlets of the stratospheric sampling experiment. Although it was not possible to document the inlet flow fields in a wind tunnel, flight tests of the experiment aboard the ER-2 indicated that the aerodynamic performance of the two-stage inlet system was very good. Measurements involved wall heating of the entry portion of both inlets and evaluation of boundary-layer growth by means of low-mass thermistors arrayed at three downstream stations and at various distances off the walls. Both primary and secondary ducts were equipped with throttling valves and velocity sensors. In-flight testing at throttle settings appropriate for the design duct velocity, and at moderate variations of velocity, indicated no wall interaction with the core flow to a distance of at least 17 diameters down the secondary duct, that is, past the test station.

The two-stage inlet design would also lend itself well to airborne aerosol sampling, because the flow that enters the test section comes from the center of the primary duct, and does not pass close to the inlet lips; therefore, it does not encounter much streamline curvature except for curvature caused by the probe angle of attack relative to the flight direction. Angle of attack can be minimized by anticipating local flow directions and orienting the probe close to the local streamwise direction, as discussed in the section on inlet design.

Internal Components

For aerosol sampling, flow curvature must be minimized because aerosols have inertia that causes them to cross curving streamlines, as discussed above. This makes it necessary to keep a straight duct between the inlet and measurement station. The use of probes with elbows upstream of the measurement station will surely lead to the introduction of circulating flow in the elbow and possibly to contact of the walls by the gas or aerosols. Figure 9 shows typical flow patterns in elbows that have no turning vanes. The momentum of the flow will drive the flow outward across the core, which will establish secondary flow vortices that rotate as shown. The fluid elements follow a helical path while negotiating the corner. These general flow patterns exist in circular or rectangular corners, whether the flow is turbulent or laminar. Corner vanes can prevent this pattern, as is discussed below, but the vanes themselves could be contacted by the gas or aerosol.

Care must be taken with the internal duct design to minimize the pressure drops in all sections except at the regulator valve. Otherwise, mass flow may be retarded, and back pressure may lead to flow separation and turbulence in the test section. In most flight cases, the system can be designed clean enough to pass adequate mass flow that is generated by ram pressure. In balloon drops with little forward speed, it has been necessary to incorporate a fan downstream of the test section in order to generate adequate mass flow rate in the test section (Weinstock et al., 1990).

Pressure drops occur all along the duct because of viscosity, but the primary pressure drops occur at corners, diffusers, junctions, area changes, and other perturbations in the duct. We have used the extensive data base of Idelchik (1966) for pressure-drop estimates, but there are numerous data sets in the literature on duct component pressure drop (see Blevins, 1984; Miller, 1974).

Generally speaking, unobstructed diffusers should have wall angles of approximately 3.5° or less relative to the duct axis to prevent flow separation. This criterion is only valid for smooth, parallel inflow with turbulent boundary layers on the walls. With blockage in the diffuser, such as the secondary inlet shown in figure 8, the wall angle can be increased, because the effective wall angle is given by

$$\alpha_w = \tan^{-1}\left(\frac{\sqrt{A_o} - \sqrt{A_i}}{\sqrt{\pi}\, l_{dif}}\right) \qquad (7)$$

where the areas have been reduced by the cross-sectional area of the obstruction.

In a turbulent boundary layer, the flow mixes randomly and will contact the wall. Since wall contact affects gas and aerosol properties, it is often necessary to sample flow that is outside the boundary layer. Unless there is flow separation at the inlet, it will take some distance before turbulent pipe flow will be established in the duct. Figure 10 shows the velocity distribution for laminar flow in the inlet section of a channel. A fully developed laminar pipe-flow velocity distribution does not develop until a distance of (Schlichting, 1979)

$$x = 0.03\, d\, Re \qquad (8)$$

so that for a Reynolds number (Re) of 5,000 to 10,000 x ranges from 150 to 300 pipe diameters. In flows with higher Reynolds numbers, the boundary layer will become

turbulent. Even then, it takes 25 to 100 pipe diameters for the boundary layer to spread to the centerline as established pipe flow. The variation in distances depend on wall roughness and inflow smoothness.

On a flat plate, the flow will transition from laminar to turbulent flow at a distance from the start of the plate approximately equal to

$$x = 350,000 \frac{\upsilon}{V_d} \qquad (9)$$

For the two stage inlet of figure 8, the boundary layer was laminar the entire length of the primary inlet (V_d = 60 m/sec) and only 0.5 cm thick at the downstream end 46 cm from the inlet. The secondary inlet scooped off the flow outside the boundary layer and started a new laminar boundary layer. Thus, turbulence was not a problem for the flow conditions experienced in the flight test.

As discussed above, turning vanes are essential to controlling flow circulation and the resulting pressure losses in corners. Figure 11 shows typical corner vanes designed to subdivide the flow into separate channels as a means of reducing pressure drop. Corner pressure drop with vanes can be a third or less of the pressure drop without vanes, depending on vane geometry. Airfoil vanes, for example, have less loss than thin vanes, though they are more expensive to fabricate. Blevins (1984) gives design information on vane geometry and spacing.

The largest pressure drop in the duct should occur at the regulator valve so that a range of mass flows can be controlled. Figure 12 shows total pressure-loss coefficients for various valves as a function of valve position (Miller, 1974). Figure 13 gives the loss coefficients for a fully open butterfly valve as a function of valve-thickness–to–duct-diameter ratio. These curves can be used as design guides, but the system should be calibrated in a laboratory to verify mass flow rate versus valve position.

Miller (1974) also presents empirical equations from Gardel that give the pressure loss associated with combining and dividing flows. In the stratospheric sampling system, for example, the primary and secondary flows were recombined before being exhausted out of the wing pod. By designing the confluence so that the two flows merge nearly parallel, the pressure drop can be minimized, and a suction can be induced to aid pumping in one duct or the other.

Exhaust

In the sampling system, the primary and secondary airflows were recombined and exhausted out the side of the ER-2 wing pod. A simple hole in the wing pod might have generated very unsteady flow that could have perturbed the entire duct system. Therefore, an exhaust hood was added, as shown in figure 14. The hood protects the exhaust from the airstream and turns the exhaust flow parallel to the airstream. This not only stabilizes the duct flow, but can create a small negative pressure at the exhaust, which will contribute to the system pumping. The external drag and suction pressure of the hood can be estimated from the work of Hoerner (1965) and the internal pressure drop of the hood can be estimated from the work of Rogallo (1940).

Concluding Remarks

The aerodynamic design of airborne probes for the capture of air and aerosols was discussed in terms of inlet lip design, internal duct components for minimum pressure drop, and exhaust geometry. Inlet designs that avoid sonic flow conditions on the lip and flow separation in the duct were shown, and cross-stream velocities of aerosols were expressed in terms of droplet density and diameter. A simple method for estimating wing upwash angles at probes was developed. A more elaborate method for flow computations, the NASA panel code called PMARC, was used successfully to compute streamlines around aircraft and through probes, as well as to compute the local velocity and pressure distributions in inlets. This allows orientation of the probe so as to align it with expected streamlines near the aircraft. An NACA 1–series inlet with modified lip radius, used for a stratospheric sampling experiment at high altitude and high flight speed, was described. The device has a two-stage inlet that decelerates the inflow with little disturbance to the flow through the test section. Boundary-layer growth, diffuser design, exhaust hood design, valve loss, flow junctions, and corner vane geometry were discussed.

References

Anderson, J. G.: The Absolute Concentration of $O(^3P)$ in the Earth's Stratosphere. Geophys. Res. Lett., vol. 2, no. 6, June 1975, pp. 231-234.

Ashby, D. L.; Dudley, M. R.; Iguchi, S. K.; Browne, L.; and Katz, J.: Potential Flow Theory and Operation Guide for the Panel Code PMARC. NASA TM-102851, 1990.

Baals, D. D.; Smith, N. F.; and Wright, J. B.: The Development and Application of High-Critical-Speed Nose Inlets. NACA Report 920, 1948.

Blevins, R. D.: Applied Fluid Dynamics Handbook. Van Nostrand Reinhold, N.Y., 1984.

Brune, W. H.; Weinstock, E. M.; and Anderson, J. G.: Midlatitude ClO Below 22 Km Altitude: Measurements with a New Aircraft-Borne Instrument. Geophys. Res. Lett., vol. 15, no. 2, Feb. 1988, pp. 144-147.

Brune, W. H.; Anderson, J. G.; and Chan, K. R.: In-Situ Observations of ClO in the Antarctic: ER-2 Aircraft Results from 54° S to 72° S Latitude. J. Geophys. Res., vol. 94, no. D14, Nov. 30, 1989, pp. 16,649-16,663.

Durst, F.; Melling, A.; and Whitelaw, J. H.: Principles and Practice of Laser-Doppler Anemometry. Academic Press, 1976.

Hoerner, S.: Fluid-Dynamic Drag. Published by author, 1965.

Huebert, B. J.; Lee, G.; and Warren, W. L.: Airborne Aerosol Inlet Passing Efficiency Measurement. J. Geophys. Res., vol. 95, no. D10, Sept. 20, 1990, pp. 16,369-16,381.

Idelchik, I. E. (A. Barouch, transl.): Handbook of Hydraulic Resistance. AE-tr-6630, U.S. Atomic Energy Commission, 1966.

Luidens, R. W.; and Abbott, J. H.: Incidence Angle Bounds for Lip Flow Separation of Three 13.97-Centimeter-Diameter Inlets. NASA TM X-3351, 1976.

Luidens, R. W.; Stockman, N. O.; and Diedrich, J. H.: An Approach to Optimum Subsonic Inlet Design. ASME 79-GT-51, Gas Turbine Conference and Exhibit and Solar Energy Conference, San Diego, Calif., Mar. 1979.

Miller, D. S.: Internal Flow Aspects and Circuit Design of Heating and Ventilation Systems. Von Karman Institute for Fluid Dynamics, Lecture Series 68, May 1974.

Nichols, M. R.; and Keith, A. L., Jr.: Investigations of a Systematic Group of NACA 1–Series Cowlings with and without Spinners. NACA Report 950, 1949.

Re, R. J.: An Investigation of Several NACA 1-Series Inlets at Mach Numbers from 0.4 to 1.29 for Mass-Flow Ratios near 1.0. NASA TM X-3324, 1975.

Rogallo, F. M.: Internal-Flow Systems for Aircraft. NACA Report 713, 1940.

Schlichting, H. (J. Kestin, transl.): Boundary-Layer Theory. McGraw-Hill Book Co., N.Y., 1979.

Seddon, J.; and Goldsmith, E. L.: Intake Aerodynamics. J. S. Przemieniecki, ed., AIAA , N.Y., and Collins Professional and Technical Books, London, 1985.

Weinstock, E. M.; Schwab, J. J.; Nee, J. B.; Schwab, M. J.; and Anderson, J. G.: A Cryogenically Cooled Photofragment Fluorescence Instrument for Measuring Stratospheric Water Vapor. Rev. Sci. Instrum., vol. 61, no. 5, May 1990, pp. 1413-1432.

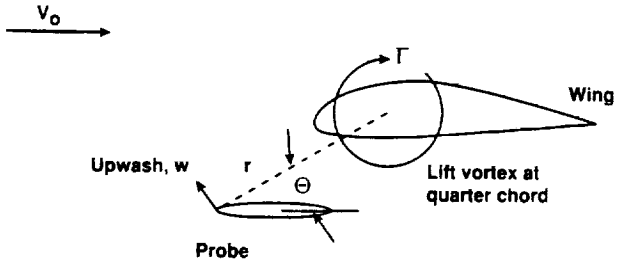

Figure 1. Geometry for wing upwash calculation using a lift vortex to simulate wing.

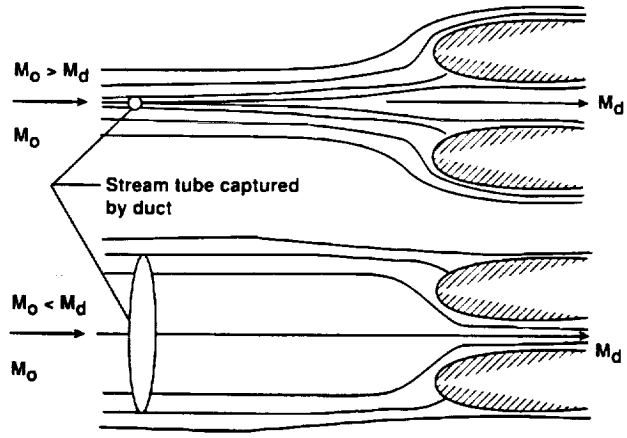

Figure 3. Inlet streamlines for flight Mach numbers greater or less than duct Mach number.

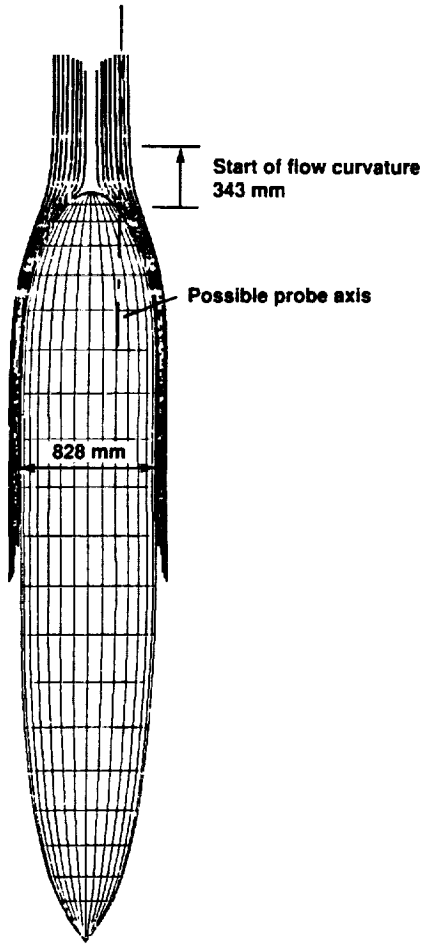

Figure 2. Predicted streamlines around ER-2 spear pod nose using PMARC; wing upwash not included.

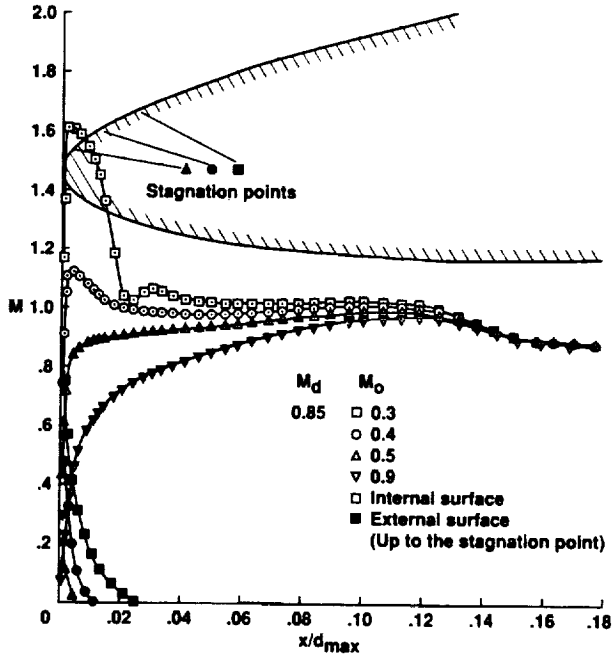

Figure 4. Effect of forward speed on lip-surface Mach number distribution (ellipse ratio 5, contraction ratio 1.15). (Seddon and Goldsmith, 1985)

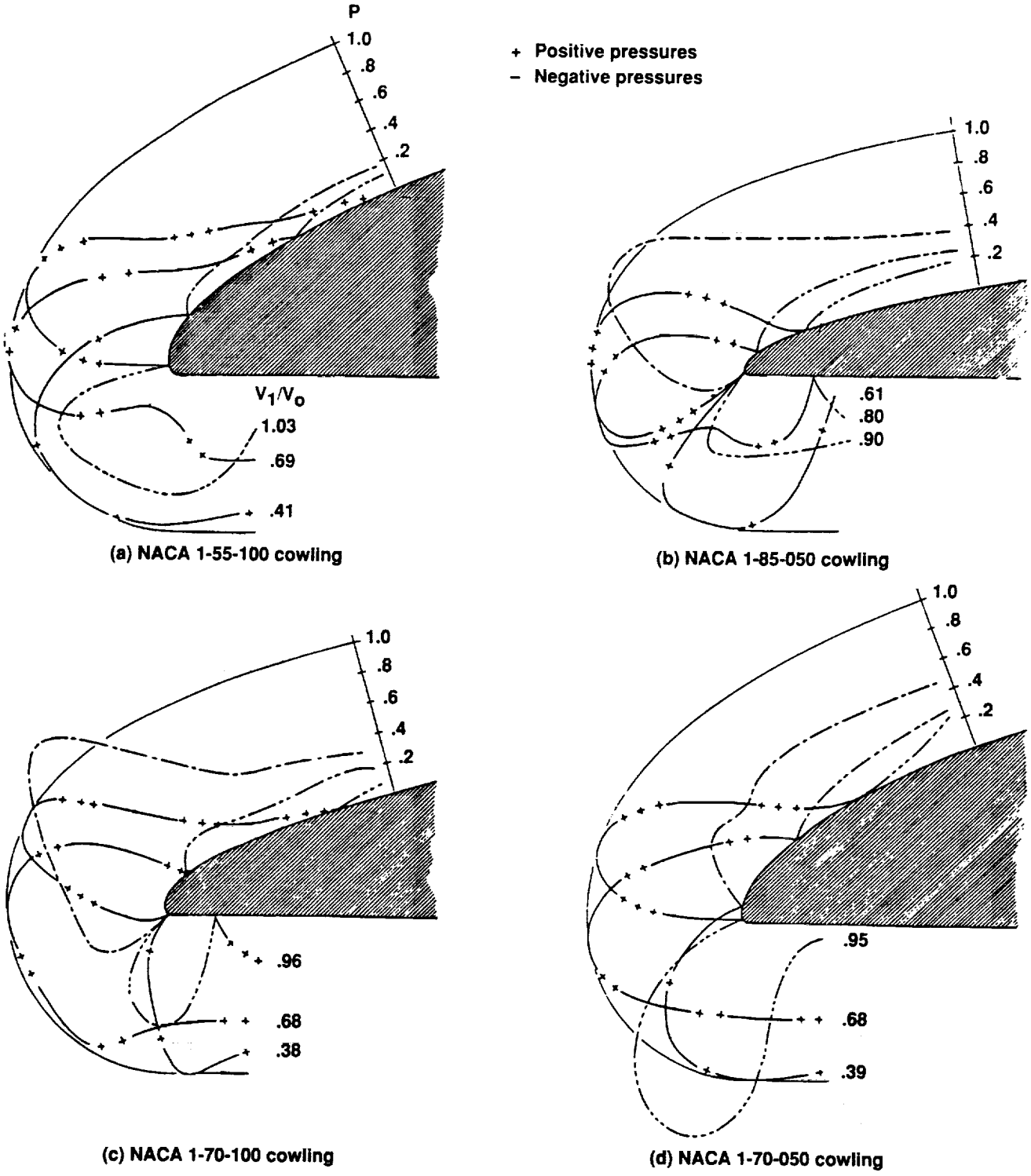

Figure 5. Static-pressure distributions around nose sections of representative NACA 1–series cowlings. Propeller removed; no spinner; $\alpha = 0°$; $M = 0.13$. (Nichols and Keith, 1949)

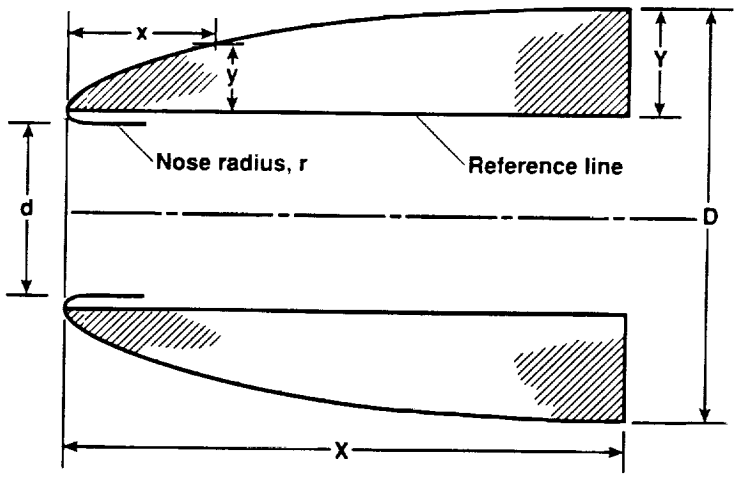

$$X = \left(\frac{X}{D}\right) D$$

$$Y = \frac{D - d}{2} - r$$

$$\text{For } r = 0.025\ Y{:}Y = \frac{D - d}{2.05} = \frac{D\left(1 - \frac{d}{D}\right)}{2.05}$$

x/X	y/Y	x/X	y/Y	x/X	y/Y	x/X	y/Y
0	0	13.0	41.94	34.0	69.08	60.0	89.11
.2	4.80	14.0	43.66	35.0	70.08	62.0	90.20
.4	6.63	15.0	45.30	36.0	71.05	64.0	91.23
.6	8.12	16.0	46.88	37.0	72.00	66.0	92.20
.8	9.33	17.0	48.40	38.0	72.94	68.0	93.11
1.0	10.38	18.0	49.88	39.0	73.85	70.0	93.95
1.5	12.72	19.0	51.31	40.0	74.75	72.0	94.75
2.0	14.72	20.0	52.70	41.0	75.63	74.0	95.48
2.5	16.57	21.0	54.05	42.0	76.48	76.0	96.16
3.0	18.31	22.0	55.37	43.0	77.32	78.0	96.79
3.5	19.94	23.0	56.66	44.0	78.15	80.0	97.35
4.0	21.48	24.0	57.92	45.0	78.95	82.0	97.87
4.5	22.96	25.0	59.15	46.0	79.74	84.0	98.33
5.0	24.36	26.0	60.35	47.0	80.50	86.0	98.74
6.0	27.01	27.0	61.52	48.0	81.25	88.0	99.09
7.0	29.47	28.0	62.67	49.0	81.99	90.0	99.40
8.0	31.81	29.0	63.79	50.0	82.69	92.0	99.65
9.0	34.03	30.0	64.89	52.0	84.10	94.0	99.85
10.0	36.13	31.0	65.97	54.0	85.45	96.0	99.93
11.0	38.15	32.0	67.03	56.0	86.73	98.0	99.98
12.0	40.09	33.0	68.07	58.0	87.95	100.0	100.00

Nose radius: 0.025Y

NOSE-INLET DESIGNATION

A designation system for nose inlets has been devised that incorporates the following basic proportions (see sketch):

- d inlet diameter
- D maximun outside diameter of nose inlet
- X length of nose inlet, measured from inlet to maximum-diameter station

The number designation is written in the form 1-40-150. The first number in the designation represents the series; the number 1 has been assigned to the present series. The second group of numbers specifies the inlet diameter in percent of maximum diameter d/D; the third group of numbers specifies the nose-inlet length in percent of maximum diameter X/D. The NACA 1-40-150 nose inlet, therefore, has a 1-series basic profile with $\frac{d}{D} = 0.40$ and $\frac{X}{D} = 1.50$.

Figure 6. NACA 1-55-100 cowling coordinates.

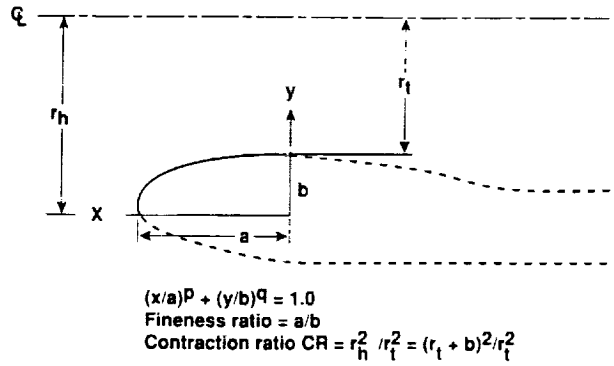

Figure 7. Elliptical lip shape parameters. (Luidens et al., 1979)

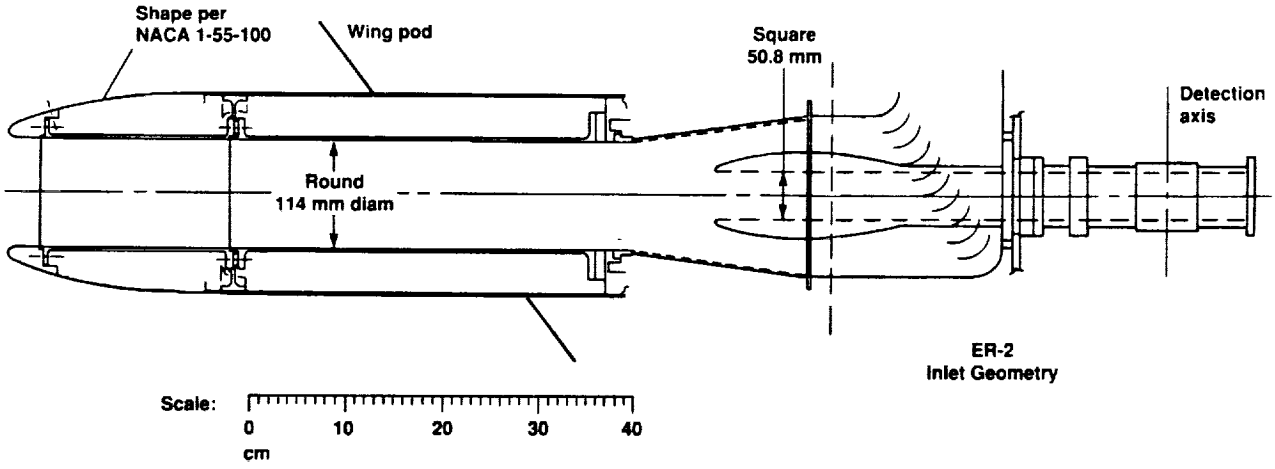

Figure 8. Two-stage inlet geometry using an NACA 1-55-100 cowling with modified lip radius.

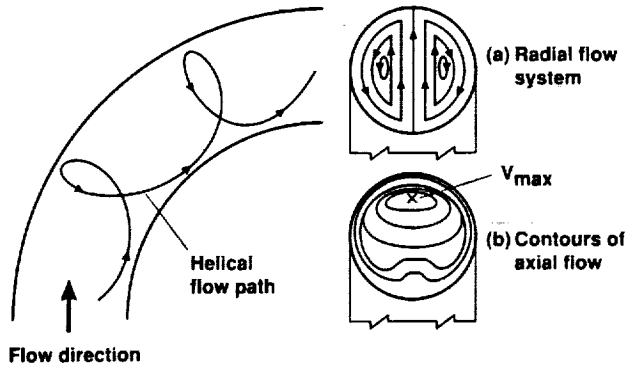

Figure 9. Flow in a curved pipe showing helical flow pattern of a fluid element and two vortices created. (Blevins, 1984)

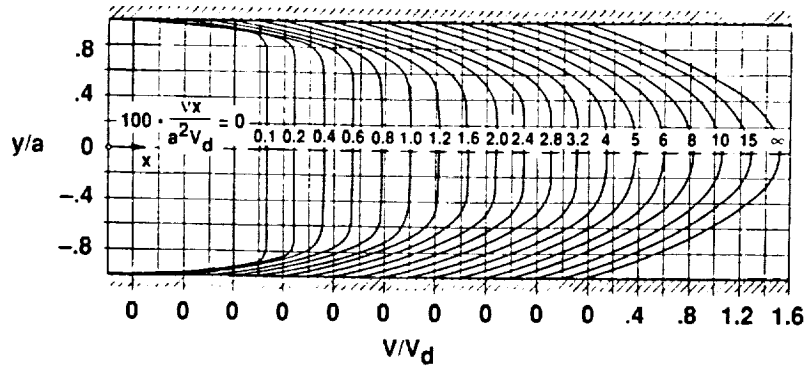

Figure 10. Velocity distribution for laminar flow in inlet section of channel (a = half channel width). (Schlichting, 1979)

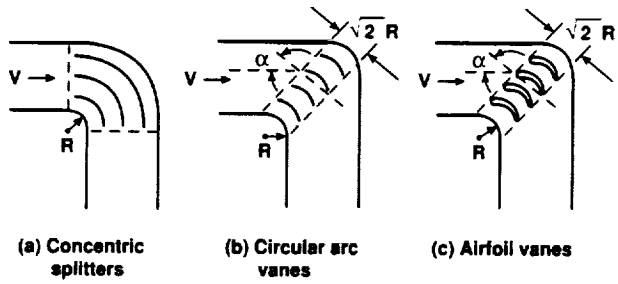

Figure 11. Three-vane systems for reducing pressure loss in sharp bends shown in a 90° bend. Angle of attack (α) is one-half the bend angle for circular-arc vanes and slightly greater for profile and airfoil vanes (R = corner radius). (Blevins, 1984)

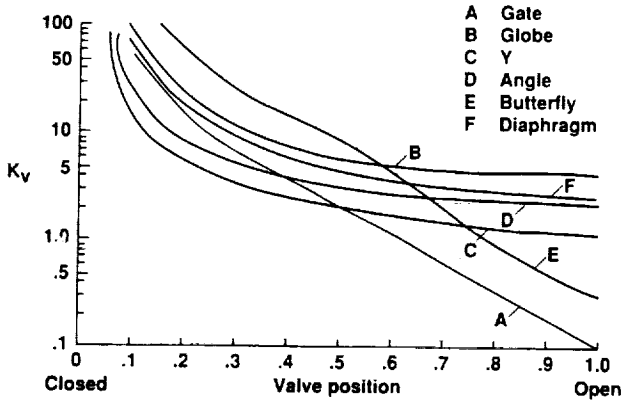

Figure 12. Total pressure loss coefficients for several duct valve types. (Miller, 1974)

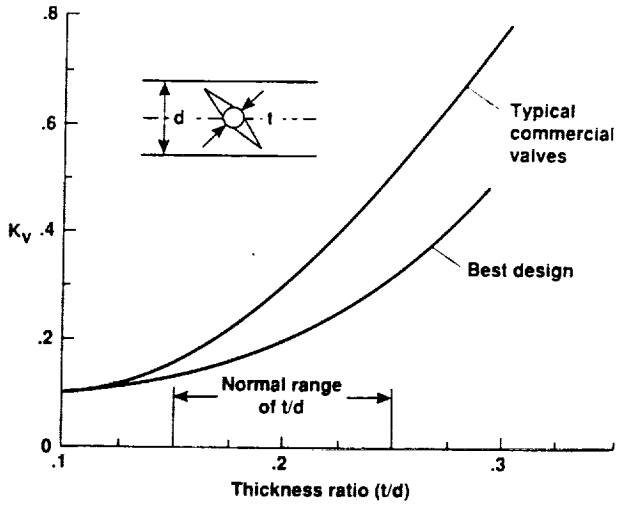

Figure 13. Total pressure loss coefficients for fully open butterfly valves. (Miller, 1974)

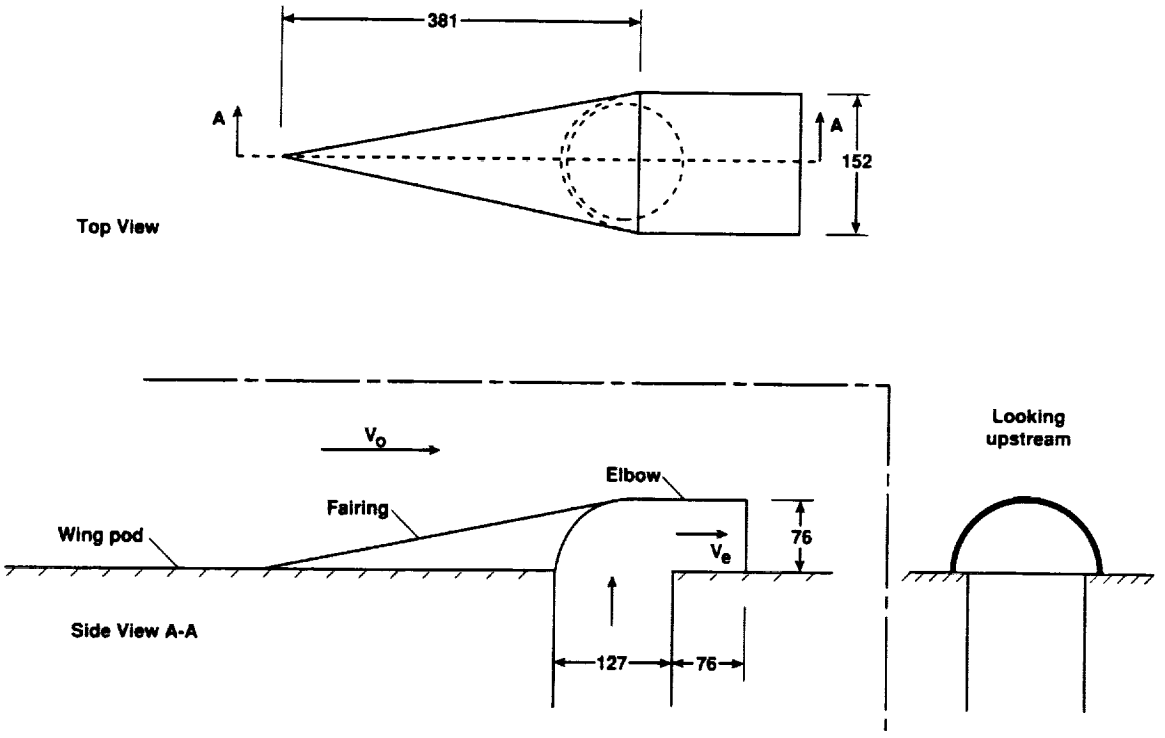

Figure 14. Exhaust hood geometry; all dimensions in mm.

REPORT DOCUMENTATION PAGE

Form Approved
OMB No. 0704-0188

Public reporting burden for this collection of information is estimated to average 1 hour per response, including the time for reviewing instructions, searching existing data sources, gathering and maintaining the data needed, and completing and reviewing the collection of information. Send comments regarding this burden estimate or any other aspect of this collection of information, including suggestions for reducing this burden, to Washington Headquarters Services, Directorate for information Operations and Reports, 1215 Jefferson Davis Highway, Suite 1204, Arlington, VA 22202-4302, and to the Office of Management and Budget, Paperwork Reduction Project (0704-0188), Washington, DC 20503.

1. AGENCY USE ONLY *(Leave blank)*	2. REPORT DATE	3. REPORT TYPE AND DATES COVERED
	September 1991	Technical Memorandum

4. TITLE AND SUBTITLE

Aerodynamic Design of Gas and Aerosol Samplers for Aircraft

5. FUNDING NUMBERS

RTOP 505-59-52

6. AUTHOR(S)

Paul T. Soderman, Nathan L. Hazen (Harvard University, Cambridge, Massachusetts), and William H. Brune (Pennsylvania State University, University Park, Pennsylvania)

7. PERFORMING ORGANIZATION NAME(S) AND ADDRESS(ES)

Ames Research Center
Moffett Field, CA 94035-1000

8. PERFORMING ORGANIZATION REPORT NUMBER

A-91110

9. SPONSORING/MONITORING AGENCY NAME(S) AND ADDRESS(ES)

National Aeronautics and Space Administration
Washington, DC 20546-0001

10. SPONSORING/MONITORING AGENCY REPORT NUMBER

NASA TM-103854

11. SUPPLEMENTARY NOTES

Point of Contact: Paul T. Soderman, Ames Research Center, MS 247-2, Moffett Field, CA 94035-1000; (415) 604-6675 or FTS 464-6675

12a. DISTRIBUTION/AVAILABILITY STATEMENT

Unclassified — Unlimited
Subject Category 47

12b. DISTRIBUTION CODE

13. ABSTRACT ***(Maximum 200 words)***

The aerodynamic design of airborne probes for the capture of air and aerosols is discussed. Emphasis is placed on the key parameters that affect proper sampling, such as inlet-lip design, internal duct components for low pressure drop, and exhaust geometry. Inlet designs that avoid sonic flow conditions on the lip and flow separation in the duct are shown. Cross-stream velocities of aerosols are expressed in terms of droplet density and diameter. Flow curvature, which can cause aerosols to cross streamlines and impact on probe walls, can be minimized by means of a proper inlet shape and proper probe orientation, and by avoiding bends upstream of the test section. A NASA panel code called PMARC has been used successfully to compute streamlines around aircraft and probes, as well as to compute the local velocity and pressure distributions in inlets. An NACA 1–series inlet with modified lip radius has been used for the airborne capture of stratospheric chlorine monoxide at high altitude and high flight speed. The device has a two-stage inlet that decelerates the inflow with little disturbance to the flow through the test section. Diffuser design, exhaust hood design, valve loss, and corner vane geometry are discussed.

14. SUBJECT TERMS

Aerosols, Gas sampling, Inlet design, Airborne sampling, Atmospheric science

15. NUMBER OF PAGES

14

16. PRICE CODE

A02

17. SECURITY CLASSIFICATION OF REPORT	18. SECURITY CLASSIFICATION OF THIS PAGE	19. SECURITY CLASSIFICATION OF ABSTRACT	20. LIMITATION OF ABSTRACT
Unclassified	Unclassified		